

# Positron stopping power in some biological compounds for intermediate energies with generalized oscillator strength model

## Abstract

In this study total inelastic differential cross section and related stopping power expressions for positron were obtained by using generalized oscillator strength model. The stopping powers of low atomic number targets and of some biological compounds for positrons were calculated over the energy range from 50 eV to 10 MeV. Calculations of the stopping powers (SPs) for some low atomic number targets: H<sub>2</sub>, C, N<sub>2</sub>, O<sub>2</sub>, P and for biological compounds: C<sub>5</sub>H<sub>5</sub>N<sub>5</sub> (adenine), C<sub>5</sub>H<sub>5</sub>N<sub>3</sub>O (guanine), C<sub>5</sub>H<sub>5</sub>N<sub>3</sub>O (cytosine), C<sub>5</sub>H<sub>6</sub>N<sub>2</sub>O<sub>2</sub> (thymine), C<sub>20</sub>H<sub>27</sub>N<sub>7</sub>O<sub>13</sub>P<sub>2</sub> (cytosine-guanine), and C<sub>19</sub>H<sub>26</sub>N<sub>8</sub>O<sub>13</sub>P<sub>2</sub> (thymine-adenine), have been evaluated for incident positrons in the 50 eV-10 MeV energy range. A detailed comparison of the calculated results with the other theoretical and experimental data for these target materials were presented. The calculated results of stopping powers for positrons in energy range from 50 eV to 10 MeV were found to be in good agreement to within 5% above 100 eV energies with other theoretical results.

**Keywords:** positron stopping power, generalized oscillator strength, biological compounds, bragg rule

Volume 3 Issue 3 - 2018

Hasan Gumus,<sup>1</sup> Tuba Namdar,<sup>1</sup> Abdelouahab Bentabet<sup>2</sup>

<sup>1</sup>Department of Physics, Faculty of Science and Arts, Ondokuz Mayıs University, Turkey

<sup>2</sup>LCVRN, Bordj Bou Arreridj University, Algeria

**Correspondence:** Hasan Gumus, Department of Physics, Faculty of Science and Arts, Ondokuz Mayıs University, 55139 Samsun, Turkey, Tel+90362312 1919/5061, Fax+90 362 457 6081, Email hgumus@omu.edu.tr

**Received:** January 26, 2018 | **Published:** May 01, 2018

## Introduction

Stopping powers (SPs) of matter for positrons are important in wide variety of applications such as nuclear medicine, radiology, basic particle physics, health physics, and radiation dosimeters design. Positron stopping powers (PSPs) at energies above 10 keV are theoretically well described and can be found in tables given in Berger & Seltzer<sup>1</sup> and the ICRU 37 Report.<sup>2</sup> The stopping power formula for positrons obtained by Batra<sup>3</sup> had been fitted by a two-parameter approximation and is valid for the energy range from 1 keV to 500 keV. On the other hand, Meiring et al.,<sup>4</sup> developed a theory of multiple scattering, exhibiting differences between positrons and electrons in the interaction with matter for the MeV energy range. In recent years there have been many studies on positron stopping power and its applications.<sup>5-8</sup>

We obtained, in a previous study<sup>9</sup> the SP formula for intermediate energy electrons, by using the generalized oscillator strength (GOS) model. Stopping power Calculations for positrons have not been studied as much, though their tracks in matter are frequently assumed to be similar to those of electrons. Positrons are used for imaging purposes (for example, PET), but can also be used for cancer therapy.<sup>10</sup> Hence, it is important to obtain SP values, for many applications in the lower energy range (<1 keV). The purpose of this study is actually to obtain a SP formula for incident positrons, valid for the low and intermediate energy region (<10 keV). The PSP formula given in this study is based on the Generalized Oscillator Strength (GOS) model<sup>11</sup> and a modification of it using the effective electron number (EEN) and effective mean excitation energies (EMEEs). In this PSP formula, analytical expressions obtained in the previous work<sup>12,13</sup> for the EEN and EMEE of target atoms are used. Thus the obtained calculating procedure was applied to evaluate the stopping power (SP) values for incoming positrons on hydrogen, carbon, nitrogen, phosphorus, and liquid

water targets. For positrons at low energies the inelastic interaction characteristics, stopping power, can not be obtained directly from Bethe's PSP theory or from experiments, which gives accurate PSPs at energies larger than 10 keV. At lower energies the theory is, in general, invalid. For low energy positrons a method used way to estimate the mentioned characteristic are dielectric theoretical methods, based on the use of the complex dielectric function  $\epsilon(q, \omega)$ ,  $m$  and  $m'$  being the momentum and energy transfer. To calculate the stopping power, other method is to make use of the inelastic differential cross section suggested by Inokuti<sup>11</sup> with Generalized Oscillator Strength (GOS). Actually, the GOS model has to be calculated from matrix elements that involve numerical integration of atomic wave functions. The aim of this study is to obtain stopping power and total inelastic differential cross section expressions for positron using the GOS model for biological compounds, valid for low and intermediate energies. Applying the GOS model, analytical expressions for the calculation of stopping Powers (SPs) have been given for biological targets. In this study total inelastic differential cross sections and stopping power expressions for positron were obtained by using Generalized Oscillator Strength (GOS) model. The calculated results of PSPs of the biological compounds, have been compared with the theoretical and semiempirical results. In addition, using the described model in this study, the PSPs for some important biological compounds (C<sub>5</sub>H<sub>5</sub>N<sub>5</sub> (adenine), C<sub>5</sub>H<sub>5</sub>N<sub>3</sub>O (cytosine), C<sub>20</sub>H<sub>27</sub>N<sub>7</sub>O<sub>13</sub>P<sub>2</sub> (cytosine-guanine), C<sub>5</sub>H<sub>5</sub>N<sub>3</sub>O (guanine), C<sub>5</sub>H<sub>6</sub>N<sub>2</sub>O<sub>2</sub> (thymine), and C<sub>19</sub>H<sub>26</sub>N<sub>8</sub>O<sub>13</sub>P<sub>2</sub> (thymine-adenine)) have been calculated (Table 1).

## Theory

In inelastic interactions the target atom is either excited to a suitable higher level than the ground level or it is ionized depending on the energy that the arriving particle imparts to the target atom.

**Table 1** SPs (MeVcm<sup>2</sup>/g) for 1-C<sub>5</sub>H<sub>5</sub>N<sub>5</sub> (adenine), 2-C<sub>4</sub>H<sub>5</sub>N<sub>3</sub>O (cytosine), 3-C<sub>5</sub>H<sub>5</sub>N<sub>5</sub>O (guanine), 4-C<sub>5</sub>H<sub>6</sub>N<sub>2</sub>O<sub>2</sub> (thymine), 5-C<sub>20</sub>H<sub>27</sub>N<sub>7</sub>O<sub>13</sub>P<sub>2</sub> (cytosine-guanine), 6-C<sub>19</sub>H<sub>26</sub>N<sub>8</sub>O<sub>13</sub>P<sub>2</sub> (thymine-adenine) and 7- H<sub>2</sub>O (liquid water). Bold figures are the data of lower accuracy.

| <b>Enerji (eV)</b> | <b>1-<br/>Adenine</b> | <b>2-<br/>Cytosine</b> | <b>3-<br/>Guanine</b> | <b>4-<br/>Thymine</b> | <b>5-<br/>cytosine-guanine</b> | <b>6-<br/>thymine-adenine</b> | <b>7-<br/>Liquid water</b> |
|--------------------|-----------------------|------------------------|-----------------------|-----------------------|--------------------------------|-------------------------------|----------------------------|
| 50                 | 608.44                | 551.57                 | 544.02                | 503.54                | 425.85                         | 429.94                        | 287.54                     |
| 60                 | 596.07                | 598.07                 | 577.46                | 594.73                | 549.58                         | 553.25                        | 639.45                     |
| 70                 | 575.44                | 578.56                 | 559.63                | 576.07                | 534.1                          | 537.32                        | 625.72                     |
| 80                 | 552.43                | 556.21                 | 538.69                | 554.32                | 515.12                         | 517.99                        | 606.35                     |
| 90                 | 529.39                | 533.59                 | 517.27                | 532.13                | 495.35                         | 497.93                        | 585.1                      |
| 100                | 507.34                | 511.78                 | 496.48                | 510.64                | 475.98                         | 478.34                        | 563.74                     |
| 200                | 355.27                | 359.69                 | 350.05                | 359.71                | 337.24                         | 338.52                        | 404.08                     |
| 300                | 276.5                 | 280.31                 | 273.11                | 280.55                | 267.64                         | 268.54                        | 317.09                     |
| 400                | 228.49                | 231.81                 | 225.99                | 232.12                | 223.39                         | 224.1                         | 263.22                     |
| 500                | 195.92                | 198.85                 | 193.94                | 199.17                | 192.41                         | 192.99                        | 226.36                     |
| 600                | 172.21                | 174.84                 | 170.58                | 175.16                | 169.67                         | 170.17                        | 199.38                     |
| 700                | 154.1                 | 156.5                  | 152.71                | 156.81                | 152.21                         | 152.64                        | 178.71                     |
| 800                | 144.37                | 146.46                 | 142.68                | 147.21                | 142.05                         | 142.64                        | 162.29                     |
| 900                | 132.89                | 134.8                  | 131.32                | 135.56                | 130.85                         | 131.41                        | 148.91                     |
| 1000               | 123.26                | 125.03                 | 121.8                 | 125.79                | 121.46                         | 121.99                        | 137.76                     |
| 2000               | 76.75                 | 77.88                  | 76.17                 | 78.27                 | 75.96                          | 76.19                         | 86.68                      |
| 3000               | 56.64                 | 57.46                  | 56.25                 | 57.73                 | 56.1                           | 56.27                         | 63.77                      |
| 4000               | 45.44                 | 46.08                  | 45.13                 | 46.3                  | 45.02                          | 45.15                         | 51.06                      |
| 5000               | 38.21                 | 38.74                  | 37.96                 | 38.92                 | 37.94                          | 38.05                         | 42.88                      |
| 6000               | 33.12                 | 33.58                  | 32.91                 | 33.74                 | 32.91                          | 33.00                         | 37.15                      |
| 7000               | 29.33                 | 29.74                  | 29.15                 | 29.88                 | 29.16                          | 29.24                         | 32.87                      |
| 8000               | 26.39                 | 26.75                  | 26.23                 | 26.88                 | 26.24                          | 26.31                         | 29.55                      |
| 9000               | 24.04                 | 24.37                  | 23.9                  | 24.48                 | 23.91                          | 23.97                         | 26.9                       |
| 10000              | 22.11                 | 22.41                  | 21.99                 | 22.51                 | 21.1                           | 22.05                         | 24.73                      |
| 20000              | 12.73                 | 12.9                   | 12.66                 | 12.96                 | 12.68                          | 12.71                         | 14.2                       |
| 30000              | 9.25                  | 9.37                   | 9.2                   | 9.41386               | 9.22                           | 9.24                          | 10.31                      |
| 40000              | 7.41                  | 7.5                    | 7.37                  | 7.53742               | 7.39                           | 7.41                          | 8.25                       |
| 50000              | 6.25                  | 6.33                   | 6.22                  | 6.35917               | 6.24                           | 6.25                          | 6.96                       |
| 60000              | 5.46                  | 5.53                   | 5.43                  | 5.55659               | 5.45                           | 5.46                          | 6.07                       |
| 70000              | 4.89                  | 4.95                   | 4.86                  | 4.97273               | 4.88                           | 4.89                          | 5.44                       |
| 80000              | 4.45                  | 4.51                   | 4.43                  | 4.5264                | 4.44                           | 4.45                          | 4.95                       |
| 90000              | 4.1                   | 4.16                   | 4.08                  | 4.18                  | 4.1                            | 4.11                          | 4.56                       |
| 100000             | 3.83                  | 3.87                   | 3.81                  | 3.89                  | 3.82                           | 3.83                          | 4.25                       |
| 200000             | 2.54                  | 2.57                   | 2.53                  | 2.58                  | 2.54                           | 2.54                          | 2.82                       |
| 300000             | 2.12                  | 2.14                   | 2.11                  | 2.15                  | 2.12                           | 2.12                          | 2.35                       |
| 400000             | 1.92                  | 1.94                   | 1.91                  | 1.95                  | 1.92                           | 1.92                          | 2.13                       |
| 500000             | 1.81                  | 1.83                   | 1.8                   | 1.84                  | 1.8                            | 1.81                          | 2                          |
| 600000             | 1.74                  | 1.76                   | 1.73                  | 1.77                  | 1.74                           | 1.74                          | 1.93                       |
| 700000             | 1.7                   | 1.72                   | 1.69                  | 1.73                  | 1.7                            | 1.7                           | 1.89                       |
| 800000             | 1.67                  | 1.69                   | 1.66                  | 1.7                   | 1.67                           | 1.68                          | 1.89                       |
| 900000             | 1.66                  | 1.68                   | 1.65                  | 1.68                  | 1.66                           | 1.66                          | 1.83                       |
| 1000000            | 1.65                  | 1.67                   | 1.63                  | 1.67                  | 1.65                           | 1.65                          | 1.82                       |

Consider a positron (mass  $m$ , charge  $+e$ ), moving with velocity  $v$ . IDCS) obtained from the first Born approximation is given by Inokuti<sup>11</sup> & Bichsel<sup>14</sup> as

$$\frac{d^2\sigma}{dQdW} = \chi \frac{1}{QW} \frac{df(Q,W)}{dW} \quad (1)$$

where  $\chi = 2\pi e^4 / mc^2 \beta^2$ ,  $W$  is energy loss and  $Q$  is the recoil energy given as

$$Q = q^2 / 2m = 2E - W - 2\sqrt{E(E-W)} \cos \theta. \quad (2)$$

$Q$  is normally used instead of the momentum transfer  $q$  or the angular deflection  $\theta$ ;  $E$  is the kinetic energy of the incident particle. The function  $df(Q,W)/dW$  is the generalized oscillator strength (GOS), which is described in detail by Inokuti.<sup>11</sup> The GOS can be represented as a surface over the plane ( $Q, W$ ), known as the Bethe surface, is defined as

$$\frac{df(Q,W)}{dW} \equiv \frac{W}{Q} \left\langle \Psi \left| \sum_{j=1}^Z \exp(iq.r_j / \hbar) \right| \Psi_0 \right\rangle^2 \quad (3)$$

where  $\Psi_0$  and  $\Psi$  are the ground state and excited state atomic or molecular wave functions, respectively, and the sum runs over the  $Z$  electrons in the target.

The total IDCS can be written as follows.<sup>15</sup>

$$\sigma^n = \int_0^{W_{\max}} dW W^n \int_{Q_-}^{Q_+} dQ \frac{d^2\sigma}{dQdW} \quad (4)$$

The recoil energies lie in the interval  $Q_- < Q < Q_+$  and  $Q_-$ , is given by Fano<sup>16</sup> as mentioned by Inokuti<sup>17</sup> as follows:

$$Q_-(E,W) = \sqrt{(mc^2)^2 + \frac{W^2}{\beta^2} - mc^2} \quad (5)$$

The stopping power is given as follows:

$$S = N\sigma^{(1)} \quad (6)$$

Here  $\sigma^{(1)}$  is the stopping cross section. The function  $df(Q,W)/dW$  is the GOS. This GOS satisfies the Bethe sum rule:<sup>11</sup>

$$\frac{1}{Z} \int_0^\infty \frac{df(Q,W)}{dW} dW = 1 \quad \text{or} \quad \sum_{i=1}^M f_i = Z \quad (7)$$

Here  $Z$  is the number of electrons per atom or molecule. The GOS is given by Liljequist<sup>18</sup> as

$$\frac{df(Q,W)}{dW} \equiv \sum_{i=1}^M f_i F(W_i; Q, W) \quad (8)$$

where  $M$ ,  $f_i$  and  $W_i$  are the number of shells, oscillator strengths for the  $i$  th shell of the target atom and  $i$  th shell resonance energies, respectively. Oscillators may be considered as the total spectrum of excitations of electrons belonging to a shell. The excitation spectrum,  $F(W_i; Q, W)$  has been suggested by Liljequist<sup>18</sup> to be written as

$$F(W_i; Q, W) = \delta(W - W_i)\theta(W_i - Q) + \delta(W - Q)\theta(Q - W_i) \quad (9)$$

where  $\delta(x)$  is the Dirac delta function and  $\theta(x)$  is a step function ( $\theta(x) = 0$  if  $x < 0$  and  $\theta(x) = 1$  if  $x \geq 0$ ).

According to Bohr<sup>19</sup> and as mentioned by Liljequist,<sup>18</sup> the inelastic excitations may be separated into two parts because of resonance-like interactions with bound electrons (inner shell) and other interactions with large momentum transfer where the atomic electrons may be considered as free. The resonance-like interactions correspond to excitations with low momentum transfer ( $Q \ll W$ ) and with energy transfers of the order of the binding energy ( $W = W_i$ ). Interactions with large momentum transfer are defined as  $Q \rightarrow 0$ ; in this region the atomic electrons are considered as rest and free.

The corresponding the OOS reduces to

$$Q \rightarrow 0 \quad \frac{df(Q=0,W)}{dW} = \frac{df(W)}{dW} \quad (10)$$

Preparation of the OOS for inner shell ionization (generally K shell) and for energy losses above  $\approx 100$  eV, has been obtained either from optical data<sup>11</sup> or by data in the X-ray region related to inner shell ionization. In this situation, the OOS is calculated by means of the relation.<sup>15,20</sup>

$$\frac{df(W)}{dW} = \frac{mc}{2\pi^2 \hbar e^2} \sigma_{ph} \quad \text{or} \quad f_k = \frac{1}{109.8 B_k} \int \sigma_{ph}(E) dE \quad (11)$$

where  $\sigma_{ph}(E)$  is the photoelectric cross section (in barns) at a given energy  $E$  (in MeV). The photoelectric cross section,  $\sigma_{ph}$ , can be obtained from experimentally based tables<sup>21</sup> or by using theoretical photoelectric cross section formulae. Other than this is a Local Plasma Approximation (LPA) of the OOS.<sup>22</sup> For several molecules, the K shell oscillator strength,  $f_k$  was calculated by means of a numerical integration (trapezoidal rule) of Eq. (11) using photoelectric cross sections given by Henke et al.,<sup>21</sup> at binding energies from 50 eV to 1 keV and for other energies (1 keV to 1 MeV) using the XCOM program produced Berger et al.,<sup>23</sup> by Akar & Gumus.,<sup>9</sup> In this paper, with the aim of checking of OOSs, we used the values of  $a$ ,  $f_k$  and  $W_v$  calculated by Akar & Gumus<sup>9</sup> and calculated the values of  $f$  and for biological targets.  $I$  for positrons. The mean ionisation energy of biological compounds were calculated from Bragg's addition rule.<sup>24</sup>

### Theoretical calculation of positron stopping powers

Excitations with  $Q=W$  which have resonance-like character can be defined as distant collisions and excitations with  $Q \neq W$  which correspond to free collisions may be referred to as close collisions.<sup>24</sup> The DCS for inelastic collisions obtained from GOS model can be split into contributions from distant longitudinal, distant transverse and close interaction,

$$\frac{d^2\sigma_{in}}{dQdW} = \frac{d^2\sigma_{d,l}}{dQdW} + \frac{d^2\sigma_{d,t}}{dQdW} + \frac{d^2\sigma_c}{dQdW} \quad (12)$$

For the case distant interactions, the CSS of electrons and positrons are the same. But positrons in matter are unstable particle that annihilate with  $s$  giving photons. Electron-positron pairs can be created if enough electromagnetic energy ( $>2mc^2$ ) is available (either from real or virtual photons). A positron does not interact with matter as a usual stable positively charged particle, since the competing process of annihilation followed by re-creation can cause the same transitions as "direct" scattering.<sup>25,26</sup> The DCS for binary collisions of positrons with free electrons at rest, obtained from the first Born approximation including the "annihilation or creation" mechanism, is given by the Bhabha<sup>27</sup> formula,

$$\frac{d^2\sigma_B}{dQdW} = \chi \frac{1}{W^2} \left[ 1 - b_1 \frac{W}{E} + b_2 \left( \frac{W}{E} \right)^2 - b_3 \left( \frac{W}{E} \right)^3 + b_4 \left( \frac{W}{E} \right)^4 \right] \delta(W - Q) \quad (13)$$

where

$$b_1 = \left( \frac{\gamma - 1}{\gamma} \right)^2 \frac{2(\gamma + 1)^2 - 1}{\gamma^2 - 1}$$

$$b_2 = \left( \frac{\gamma - 1}{\gamma} \right)^2 \frac{3(\gamma + 1)^2 + 1}{(\gamma^2 - 1)^2}$$

$$b_3 = \left( \frac{\gamma - 1}{\gamma} \right)^2 \frac{2\gamma(\gamma - 1)}{(\gamma^2 + 1)^2}$$

$$b_4 = \left( \frac{\gamma - 1}{\gamma} \right)^2 \frac{(\gamma - 1)^2}{(\gamma + 1)^2} \quad (14)$$

The DCSs for distant interactions is the sum of contributions from transverse and longitudinal interactions:

$$\frac{d\sigma_d}{dW} = \chi \sum_k f_k \left\{ \frac{1}{W} \frac{2m_e c^2}{Q(Q + 2m_e c^2)} + \frac{1}{W} \left[ \ln \left( \frac{1}{1 - \beta^2} \right) - \beta^2 - \delta_F \right] \right\} \delta(E - W_k) \theta(W_k - Q) \quad (15)$$

Using Eq. (13) and Eq. (14), total inelastic differential cross section are given with following expression:

$$\sigma_{in}^{(1)} = \chi$$

$$\sum_k f_k \left\{ \ln \left( \frac{W_k Q + 2m_e c^2}{Q - W_k + 2m_e c^2} \right) + \ln \left( \frac{1}{1 - \beta^2} \right) - \beta^2 - \delta_F + \frac{1}{W} \left[ 1 - b_1 \frac{W}{E} + b_2 \left( \frac{W}{E} \right)^2 - b_3 \left( \frac{W}{E} \right)^3 + b_4 \left( \frac{W}{E} \right)^4 \right] \right\} \Theta(W_{max} - W_k) \quad (16)$$

By using Eq. (6) and Eq. (16), and taking  $W_{max} = E$ , SP for positrons can be written as follow,

$$S(E) = N\chi$$

$$\sum_k f_k \left\{ \ln \left( \frac{W_k Q + 2m_e c^2}{Q - W_k + 2m_e c^2} \right) + \ln \left( \frac{1}{1 - \beta^2} \right) - \beta^2 - \delta_F + \frac{1}{W} \left[ 1 - b_1 \frac{W}{E} + b_2 \left( \frac{W}{E} \right)^2 - b_3 \left( \frac{W}{E} \right)^3 + b_4 \left( \frac{W}{E} \right)^4 \right] \right\} \Theta(W_{max} - W_k) \quad (17)$$

For positrons the SP of compounds were calculated from Bragg's addition rule<sup>24</sup> as follows:

$$\frac{S(E)}{\rho} (\text{compound}) = \sum_i w_i \left[ \frac{S(E)}{\rho} \right]_i \quad (18)$$

where  $w_i$  are the atomic fractions in molecule.

## Calculated results and discussion

In this study, to obtain the inelastic SPs for positrons of biological materials the OS of the inner and valence shell PMIPs,  $W_i$  and  $W_v$ , calculated by Akar & Gumus<sup>9</sup> were used in Eq. (17). The calculated PSPs for H<sub>2</sub>, C, N<sub>2</sub>, O<sub>2</sub>, P, C<sub>5</sub>H<sub>5</sub>N<sub>5</sub> (adenine), C<sub>4</sub>H<sub>5</sub>N<sub>3</sub>O (cytosine), C<sub>20</sub>H<sub>27</sub>N<sub>7</sub>O<sub>13</sub>P<sub>2</sub> (cytosine-guanine), C<sub>5</sub>H<sub>5</sub>N<sub>5</sub>O (guanine), C<sub>5</sub>H<sub>6</sub>N<sub>2</sub>O<sub>2</sub> (thymine), C<sub>19</sub>H<sub>26</sub>N<sub>8</sub>O<sub>13</sub>P<sub>2</sub> (thymine-adenine) and liquis warer are given in the Figs. 1-12.

Figure 1 shows the mass stopping power (mSP) for incident positrons from 50 eV to 10 MeV energy range in hydrogen. The results obtained from this study are compared with the PENELOPE program<sup>26</sup> and results for positrons by using Gumus calculation methods.<sup>12,28</sup> The calculated PSPs values obtained by using Eqs. (17, 18) are good agreement with PENELOPE program<sup>26</sup> results to within 1% expect at energies below 100 eV.

Figure 2 shows the mSP for incident positrons from 50 eV to 10 MeV energy range in carbon. The results obtained from this study are

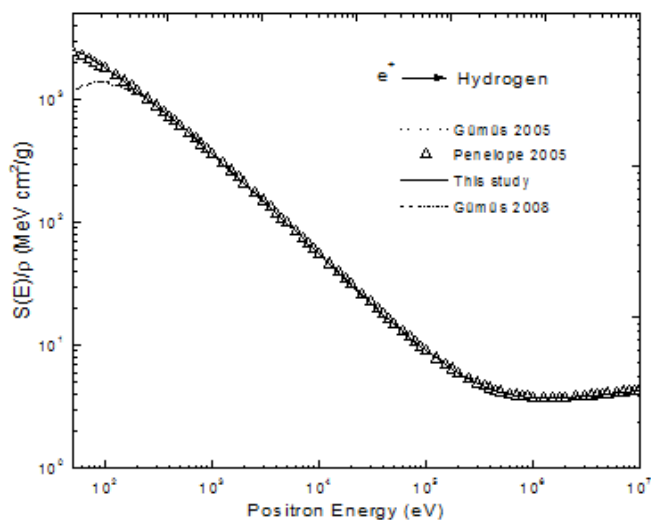
compared with the PENELOPE program,<sup>26</sup> values of ICRU 37 report and results for positrons by using Gumus calculation methods.<sup>12, 28</sup> The calculated PSPs values obtained by using Eqs. (21, 22) are good agreement with PENELOPE program<sup>26</sup> results to within 1%. expect at energies below 300 eV.

Figure 3 shows the mSP for incident positrons from 50 eV to 10 MeV energy range in nitrogen. The results obtained from this study are compared with the PENELOPE program.<sup>26</sup> and results for positrons by using Gumus calculation methods.<sup>12,28</sup> The calculated PSPs values obtained by using Eqs. (21, 22) are good agreement with PENELOPE program 26 results to within 3%.

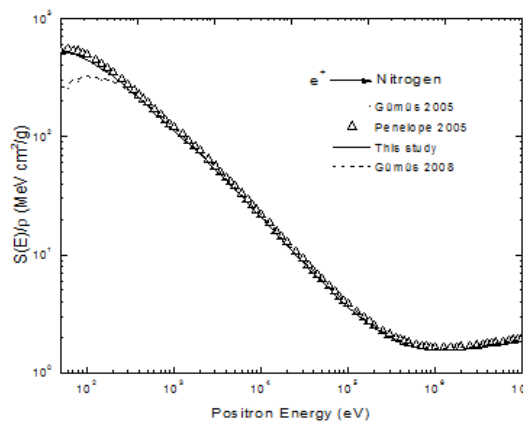
Figure 4 shows the mSP for incident positrons from 50 eV to 10 MeV energy range in oxygen. The results obtained from this study are compared with the PENELOPE program and results for positrons by using Gumus calculation methods.<sup>12,28</sup> The calculated PSPs values obtained by using Eqs. (17,18) are good agreement with PENELOPE program 26 results to within 3%.

Figure 5 shows the mSP for incident positrons from 50 eV to 10 MeV energy range in phosphorus. The results obtained from this study are compared with the PENELOPE program 26 and results for positrons by using Gümüş calculation methods.<sup>8,29</sup> The calculated PSPs values obtained by using Eqs. (17, 18) are good agreement with PENELOPE program<sup>22</sup> results to within 2%. expect at energies below 300 eV.

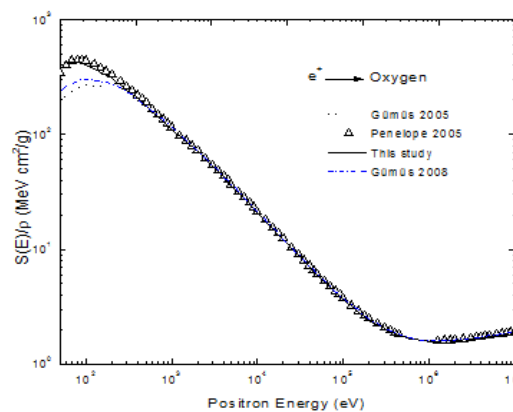
are compared with the PENELOPE program.<sup>26</sup> The calculated PSPs values obtained by using Eqs. (17,18) are good agreement with PENELOPE program results to within 3%.



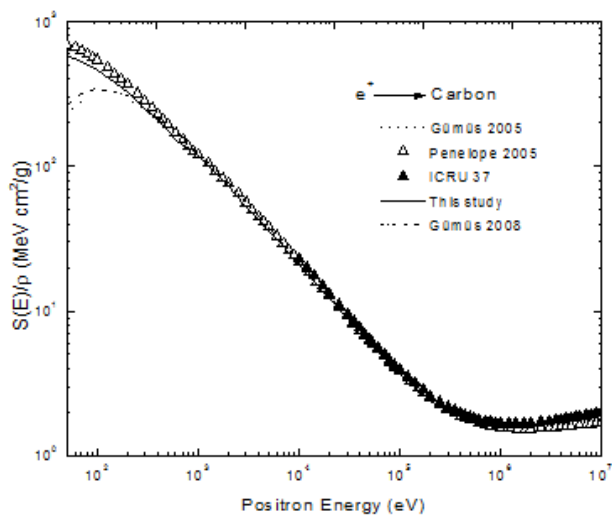
**Figure 1** Mass stopping power  $S(E)/\rho$  for incident positron energies, in H. —, present study; ..., theoretical data from Gumus<sup>12</sup>; and ----, from Gumus<sup>29</sup> model;  $\Delta$ , results calculated by PENELOPE Program.<sup>27</sup>



**Figure 3**  $S(E)/\rho$  for incident positron energies, in nitrogen; —, present study; ..., theoretical data from Gumus<sup>12</sup>; and ----, from Gumus<sup>29</sup> model;  $\Delta$ , results calculated by PENELOPE Program.<sup>27</sup>



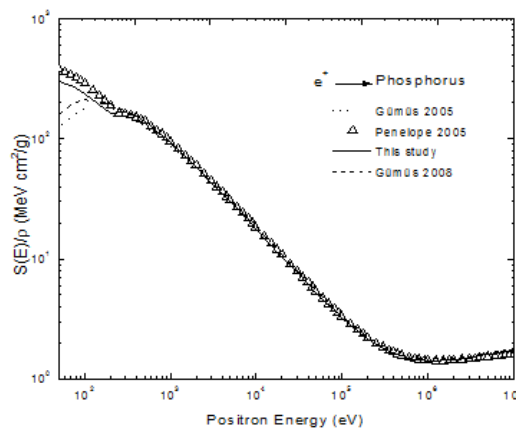
**Figure 4**  $S(E)/\rho$  for incident positron energies, in oxygen. —, present study;  $\Delta$ , results calculated by PENELOPE Program;<sup>27</sup> .... theoretical data of Gumus<sup>12</sup>; and ---- theoretical data of Gumus.<sup>29</sup>



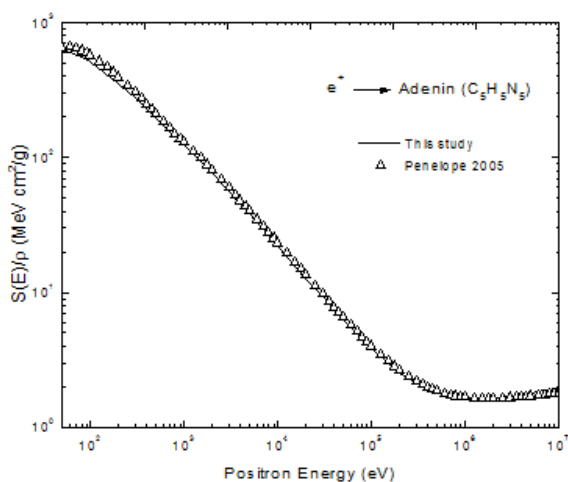
**Figure 2**  $S(E)/\rho$  for incident positron energies, in carbon. —, present study; ..., theoretical data from Gumus<sup>12</sup>; and ----, from Gumus<sup>29</sup> model;  $\Delta$ , results calculated by PENELOPE Program;<sup>27</sup>  $\blacktriangle$ , data from ICRU 37 report (1984).

Figure 6 shows the mSP for incident positrons from 50 eV to 10 MeV energy range in adenin. The results obtained from this study are compared with the PENELOPE program.<sup>26</sup> The calculated PSPs values obtained by using Eqs. (17,18) are good agreement with PENELOPE program<sup>26</sup> results to within 2%.

Figure 7 shows the mSP for incident positrons from 50 eV to 10 MeV energy range in cytosine. The results obtained from this study

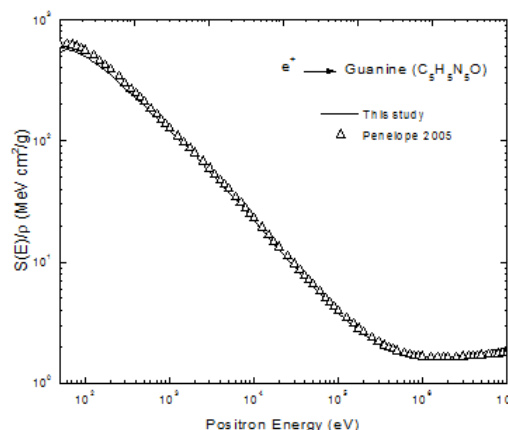


**Figure 5**  $S(E)/\rho$  for incident positron energies, in phosphorus. —, present study;  $\Delta$ , results calculated by PENELOPE Program;<sup>27</sup> .... theoretical data of Gumus<sup>8</sup>; and ---- theoretical data of Gumus.<sup>29</sup>

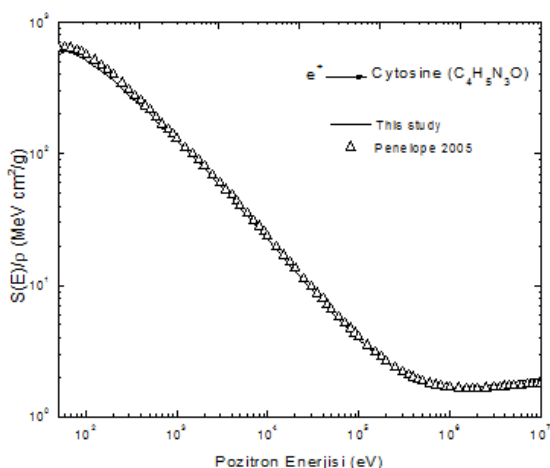


**Figure 6**  $S(E)/\rho$  for incident positron energies, in adenine. —, present study;  $\Delta$ , results calculated by PENELOPE Program.<sup>27</sup>

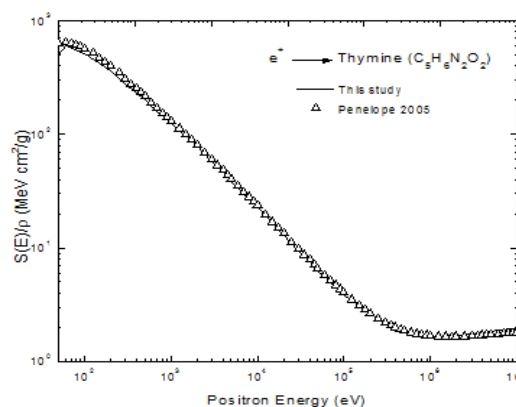
study are compared with the PENELOPE program.<sup>26</sup> The calculated PSPs values obtained by using Eqs. (17,18) are good agreement with PENELOPE program results to within 5%.



**Figure 8**  $S(E)/\rho$  for incident positron energies, in guanine. —, present study; and  $\Delta$ , PENELOPE Program<sup>27</sup> results.



**Figure 7**  $S(E)/\rho$  for incident positron energies, in cytosine. —, present study; and  $\Delta$ , PENELOPE Program results.



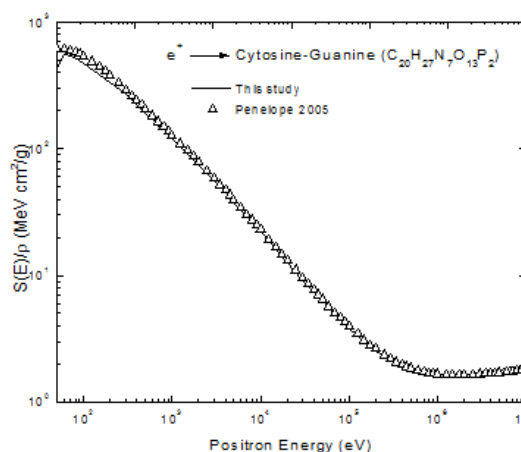
**Figure 9**  $S(E)/\rho$  for incident positron energies, in thymine. —, present study; and  $\Delta$ , PENELOPE Program<sup>27</sup> results.

Figure 8 shows the mSP for incident positrons from 50 eV to 10 MeV energy range in guanine. The results obtained from this study are compared with the PENELOPE program.<sup>26</sup> The calculated PSPs values obtained by using Eqs. (17,18) are good agreement with PENELOPE program results to within 4%.

Figure 9 shows the mSP for incident positrons from 50 eV to 10 MeV energy range in thymine. The results obtained from this study are compared with the PENELOPE program.<sup>22</sup> The calculated PSPs values obtained by using Eqs. (17,18) are good agreement with PENELOPE program results to within 5%.

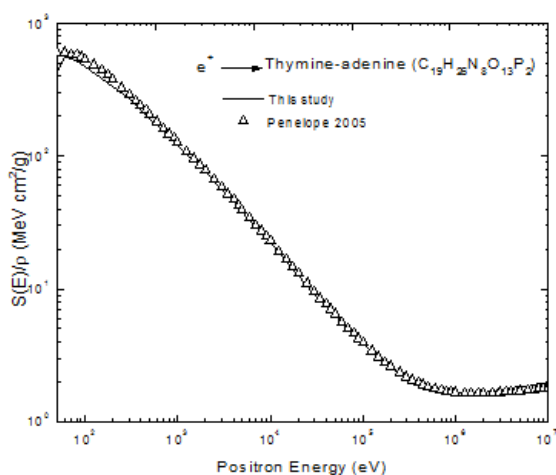
Figure 10 shows the mSP for incident positrons from 50 eV to 10 MeV energy range in cytosine-guanine. The results obtained from this study are compared with the PENELOPE program.<sup>26</sup> The calculated PSPs values obtained by using Eqs. (17,18) are good agreement with PENELOPE program results to within 5%.

Figure 11 shows the mSP for incident positrons from 50 eV to 10 MeV energy range in thymine-adenine. The results obtained from this



**Figure 10**  $S(E)/\rho$  for incident positron energies, in cytosine-guanine. —, present study; and  $\Delta$ , PENELOPE Program<sup>27</sup> results.

Figure 12 shows the mSP values for incident positrons from 50 eV to 10 MeV energy range in liquid water. The results obtained in this study are in good agreement with the recommendations of ICRU 37 (1984) for the stopping power of liquid water. The results obtained from this study are compared with the PENELOPE program<sup>26</sup> and results for positrons by using Gümüş calculation methods.<sup>12, 28</sup> The calculated PSPs values obtained by using Eqs. (17,18) are good agreement with PENELOPE program results to within 3% above 300 eV energies. The mass stopping powers obtained by using the formalism described in this paper are in good agreement to within data of predictions of Pimblott<sup>30</sup> above 500 eV energies,



**Figure 11**  $S(E)/\rho$  for incident positron energies, in thymine-adenine. —, present study; and  $\Delta$ , PENELOPE Program<sup>27</sup> results.

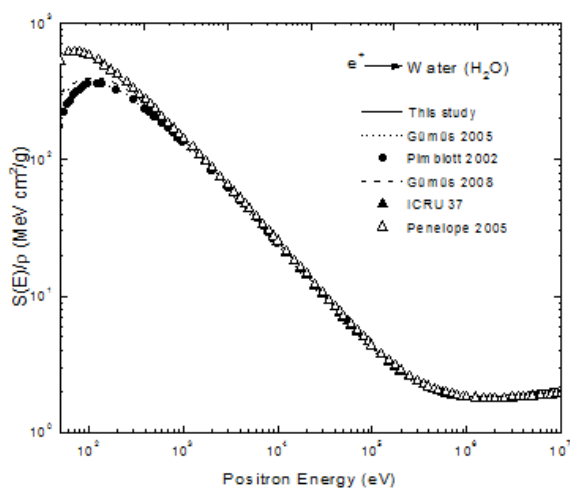


**Figure 12**  $S(E)/\rho$  for incident positron energies, in liquid water. —, present study; and  $\Delta$ , PENELOPE Program<sup>23</sup> results. .... theoretical data of Gumus<sup>12</sup>; ---- theoretical data of Gumus<sup>29</sup>; results of Pimblott<sup>30</sup> and  $\blacktriangle$ , results of ICRU 37 report.<sup>2</sup>

## Concluding remarks

In this study, the SP values for positrons in biological materials have been calculated with the GOS model. K shell oscillator strengths, the semiempirical adjustment factor  $a_s$ , K and valence shell PMIP

values and MIE values of elements have been calculated. In addition, the stopping power for the biological compounds,  $C_5H_5N_5$  (adenine),  $C_5H_5N_3O$  (guanine),  $C_4H_5N_3O$  (cytosine),  $C_{20}H_{27}N_7O_{13}P_2$  (cytosine-guanine),  $C_5H_6N_2O_2$  (thymine) and  $C_{19}H_{26}N_8O_{13}P_2$  (thymine-adenine)) have been analysed for incident positrons in the 50 eV-1 MeV energy range. The calculated results of stopping power for positrons in molecules including  $H_2$ , C,  $N_2$ ,  $O_2$ ,  $C_5H_5N_5O$  in biological targets are found to be in good agreement with semiempirical results and theoretical results. The present inelastic SPs calculations for positrons with the GOS model depends on K and valence shell strengths, K and valence shell PMIPs. The presented positron SP calculations should be useful for biological target such as  $C_5H_5N_5$  (adenine),  $C_5H_5N_3O$  (cytosine),  $C_5H_5N_3O$  (guanine),  $C_5H_6N_2O_2$  (thymine),  $C_{20}H_{27}N_7O_{13}P_2$  (cytosine-guanine) and  $C_{19}H_{26}N_8O_{13}P_2$  (thymine-adenine). In addition, the straggling formula given in this study should be use for biological compounds.

## Acknowledgement

We thank to OECD NEA Computer Program Service ([www.nea.fr](http://www.nea.fr)) for PENELOPE program 2005 and 2008.

## Conflict of interest

The author declares no conflict of interest.

## References

- Berger MJ, Seltzer SM. Stopping powers and ranges of electrons and positrons. *National Bureau of Standards*. 1982;82(2550):1–170.
- ICRU, Stopping powers for electrons and positrons. *International Commission on Radiation Units and Measurements*. 1984;37:271.
- Batra RK. *Nucl Instrum Methods*. 1987;28:195.
- Meiring WJ, Van Klinken J, Wichers VA. Rapid Communications. *Physical Review A*. 1991;44(5):2960.
- Tanir G, Bölükdemir MH, Keleş S. *Chinese Journal of Physics*. 2012;50(3):425–433.
- Blanco F, Munoz A, Almeida D, et al. Modelling low energy electron and positron tracks in biologically relevant media. *Eur Phys J*. 2013;67(199):1–18.
- Gümüş H, Kabadayi Ö, Tufan MC. Calculation of the Stopping Power for Intermediate Energy Positrons. *Chinese Journal of Physics*. 2006;44(4):290–296.
- Handrack J, Tessonnier T, Chen W, et al. Sensitivity of post treatment positron emission tomography/computed tomography to detect inter-fractional range variations in scanned ion beam therapy. *Acta Oncol*. 2017;56(11):1451–1458.
- Akar A, Gümüş H. Electron stopping power in biological compounds for low and intermediate energies with the generalized oscillator strength (GOS) model. *Radiat Phys Chem*. 2005;73(4):196–203.
- Malik E, Juweid MD, Bruce D, et al. Positron-Emission tomography and assessment of cancer therapy. *N Engl J Med*. 2006;354(5):496–507.
- Inokuti M. Inelastic Collisions of Fast Charged Particles with Atoms and Molecules—The Bethe Theory Revisited. *Rev Mod Phys*. 1971;43(3):297.
- Gümüş H. simple stopping power formula for low and intermediate energy electrons. *Radiation Physics and Chemistry*. 2005;72(1):7–12.

13. Gümüş H, Kabadayi O, Tufan MC. Calculation of the Stopping Power for Intermediate Energy Positrons. *Chinese Journal of Physics*. 2006;44(4):290.
14. Bichsel H. *Scanning Microsc. Suppl*. 1990;4:147.
15. Fernández Varea JM. *Rad Phys and Chem*. 1998;53:235.
16. Fano U, Ann. Penetration of Protons, Alpha Particles, and Mesons. *Rev Nucl Sci*. 1963;13:1–16.
17. Inokuti M. Addenda: Inelastic collisions of fast charged particles with atoms and molecules—The Bethe theory revisited. *Rev Mod Phys*. 1978;50(1):23.
18. Liljequist D. Simple generalized oscillator strength density model applied to the simulation of keV electron energy loss distributions. *J Appl Phys*. 1985;57(3):657.
19. Bohr N, *Mat Fyz. Medd Dan. Vidensk Selsk*. 1948;18(8):1.
20. Cengiz A. Approximate inelastic scattering cross sections of electrons. *Radiation Physics and Chemistry*. 2002;65(1):33–44.
21. Henke BL, Gullikson EM, Davis JC. X-Ray interactions: photo absorption, scattering, Transmission and reflection at E= 50-30,000 eV, Z=1-92. *Atomic Data and Nuclear Data Tables*. 1993;54(2):181–342.
22. Johnson RE, Inokuti M. *At Mol Phys*. 1983;14:19.
23. Berger MJ, Hubbell JH, Seltzer SM, et al. XCOM: Photon Cross Sections Data Base. *NIST*;1987.
24. Bragg WH, Kleeman R. On the  $\alpha$  particles of radium, and their loss of range in passing through various atoms and molecules. *Philos Mag*. 1905;10(57):318–340.
25. Sakurai JJ, *Advanced Quantum Mechanics*. UK: Addison-Wesley; 1967.
26. Salvat F, Fernandez Varea JM, Sempau. PENELOPE, A Code Systems for monte carlo simulation of electron and photon transport, France: NEA Databank; 2005.
27. Bhabha H. *Proc Roy Soc*. 1936;154:195.
28. Gümüş H. New stopping power formula for intermediate energy electrons. *Applied Radiation and Isotopes*. 2008;66(12):1861–1869.
29. Salvat F, Fernández Varea JM. Semiempirical cross sections for the simulation of the energy loss of electrons and positrons in matter. *Nucl Instr And Meth*. 1992;63(3):255–269.
30. Pimblott SM, Siebbeles LDA, *Nucl Instr Meth B*. 2002;194:237.